ACS chemical biology

ARTICLES

pubs.acs.org/acschemicalbiology

Ca^{2+} Regulation of Mitochondrial ATP Synthesis Visualized at the Single Cell Level

Masahiro Nakano,[†,‡] Hiromi Imamura,[†,§,⊥,*] Takeharu Nagai,[‡] and Hiroyuki Noji[†,¶,*]

[†]Institute of Scientific and Industrial Research, Osaka University, Japan

[‡]Research Institute for Electronic Science, Hokkaido University, Japan

[§]PRESTO, Japan Science and Technology Agency, Japan

[⊥]The Hakubi Project, Kyoto University, Japan

[¶]Department of Applied Chemistry, University of Tokyo, Japan

Supporting Information

ABSTRACT: Intracellular Ca^{2+} levels play a crucial role in the control of ATP synthesis. However, the spatiotemporal correlation between ATP and Ca^{2+} remains unclear due to the inability to visualize these factors within same individual cells. A Förster resonance energy transfer (FRET)-based fluorescent ATP probe, named ATeam, was recently developed for ATP imaging in single living cells. However, the spectra of cyan fluorescent protein (CFP) and yellow fluorescent protein (YFP) used as the FRET donor and the acceptor, respectively, significantly overlap with the ultraviolet-excitable Ca^{2+} probe, fura-2. In the present work, we developed new red-shifted ATP probes, GO-ATeams, in which green fluorescent protein (GFP) and orange fluorescent protein (OFP) was used as the FRET pair to minimize spectral overlap with the fura-2 emission. The dynamics of intracellular Ca^{2+} and mitochondrial ATP levels in single histamine-stimulated HeLa cells were successfully visualized by using fura-2 and GO-ATeam. The experiments showed that histamine induced increases of both intracellular Ca^{2+} and mitochondrial ATP levels. The increment of mitochondrial ATP levels was proportional to that of Ca^{2+}. This finding suggests that cellular Ca^{2+} levels might precisely control mitochondrial ATP synthesis in response to the increased ATP consumption triggered by Ca^{2+}. In addition, GO-ATeam has several advantages over the original ATeam. The GO-ATeam signal was more stable against acidification, which would allow ATP imaging inside acidic intracellular compartments. Also, the GO-ATeam excitation wavelength is much less phototoxic to cells, making the probe suitable for long-time observation.

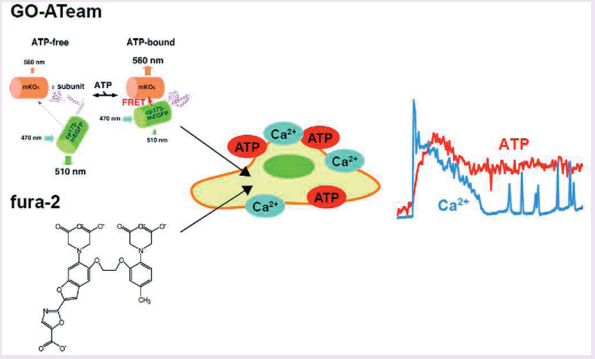

ATP is the major cellular energy currency and is involved in many biological processes, such as muscle contraction, membrane transport, intracellular trafficking, and metabolic reactions. Demand for ATP drastically changes with cellular activity. For example, the rate of ATP turnover in cardiac muscle is 5-fold higher during strenuous activity than it is at rest.[1] Therefore ATP synthesis must be strictly controlled to meet physiological demand. Otherwise, intracellular ATP would become depleted, deleteriously affecting cell functions. More than 30 years ago, Ca^{2+} was found to enhance the activity of several mitochondrial dehydrogenases, including glycerol phosphate dehydrogenase,[2] pyruvate dehydrogenase,[3] isocitrate dehydrogenase,[4] and α-ketoglutarate dehydrogenase,[5] involved in mitochondrial ATP synthesis. These findings have led to a hypothesis that elevating intracellular Ca^{2+} not only activates ATP-consuming processes but also enhances mitochondrial ATP-producing processes to maintain cellular ATP levels.[6] Cytoplasmic Ca^{2+} enters into the mitochondrial matrix, probably through the recently identified Ca^{2+} channels.[7,8] Jouaville and co-workers [9] have shown that the luminescence of either cytoplasmically or mitochondrially targeted firefly luciferase is enhanced by hormonal stimulation, suggesting hormone-induced increases in ATP levels in the cytoplasm and mitochondria. By comparing ATP dynamics, measured by luciferase luminescence, and Ca^{2+}, measured by aequorin luminescence, the group also suggested that Ca^{2+} can potentiate long-term activation of ATP synthesis in the mitochondria. However, because firefly luciferase luminescence was measured in multiple cells and because luciferase and aequorin luminescences were measured in 2 different cell populations, several questions still remain unclear. Does mitochondrial ATP concentration ($[ATP]_m$) increase in all cells with elevated Ca^{2+}? If so, is the $[ATP]_m$ increase proportional to $[Ca^{2+}]$ in each cell? Does the $[ATP]_m$ increase always follow that of $[Ca^{2+}]$? In addition, the high pH sensitivity of

Received: October 8, 2010
Accepted: April 13, 2011
Published: April 13, 2011

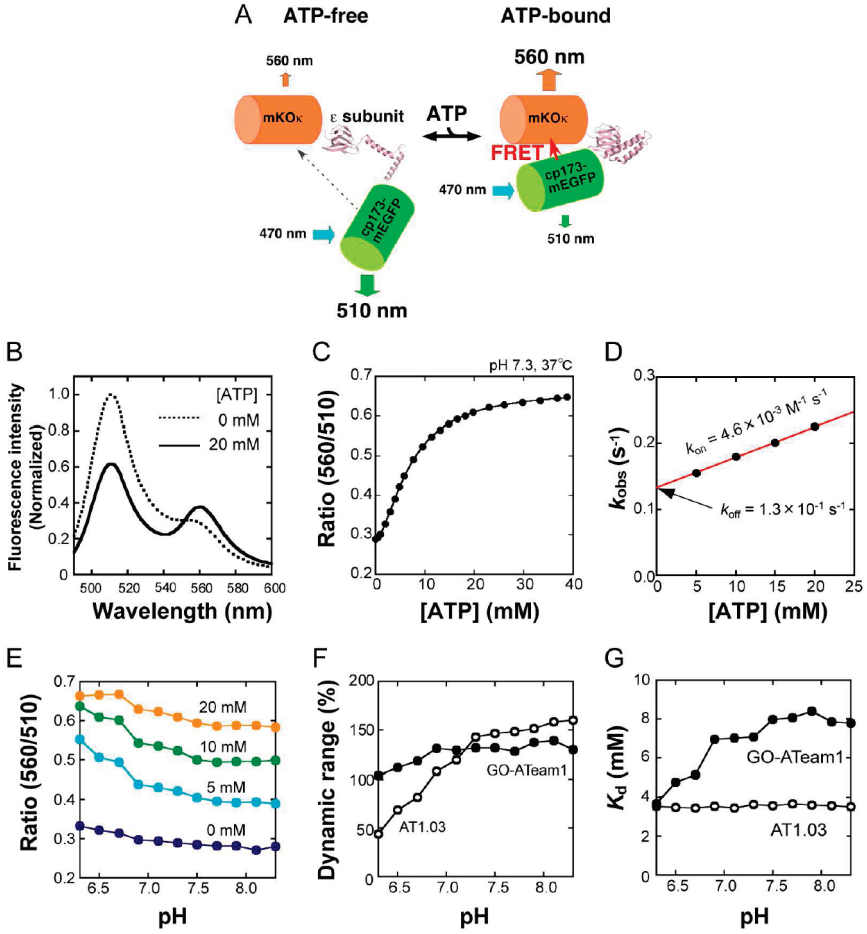

Figure 1. GFP- and OFP-based ATP probes (GO-ATeam). (A) Schematic drawing of GO-ATeam probe. Variants of green fluorescent protein (GFP; cp173-mEGFP) and orange fluorescent protein (OFP; mKOκ) were connected by the ε subunit of *Bacillus subtilis* F_oF_1-ATP synthase. In the ATP-free form (left), the extended, flexible conformation of the ε subunit separates the 2 fluorescent proteins, resulting in low FRET efficiency. In the ATP-bound form (right), the ε subunit retracts to draw the 2 fluorescent proteins close to each other, which increases FRET efficiency. (B) Fluorescence spectra of GO-ATeam1 in the absence (dotted line) and presence of ATP (20 mM, solid line) in 50 mM MOPS-KOH (pH 7.3), 50 mM KCl, 0.5 mM $MgCl_2$, and 0.05% (w/v) Triton X-100. The excitation wavelength was 470 ± 10 nm. (C) ATP-dependent fluorescent emission ratio change of GO-ATeam1 proteins *in vitro*. The change in the fraction of emission ratio (560/510 nm, R) change was plotted against ATP concentrations ([ATP]). The plot was fitted with the Hill equation: $R = (R_{max} - R_{min}) \times [ATP]^n/([ATP]^n + K_d^n) + R_{min}$, where R_{max} and R_{min} are the maximum and minimum fluorescent emission ratios, respectively, K_d is the apparent dissociation constant, and n is the Hill coefficient. (D) Reaction rate constants of GO-ATeam1. Observed rate constants ($k_{obs} = k_{on}[ATP] + k_{off}$) at 37 °C, which were determined by fitting the GFP fluorescence decrease after ATP addition with a single exponential equation, were plotted against ATP concentrations ([ATP]). Mean values of two independent measurements are shown. From a linear fit to the plot, k_{on} and k_{off} were calculated as 4.6 × 10^{-3} M^{-1} s^{-1} and 1.3 × 10^{-1} s^{-1}, respectively. (E) pH-dependent fluorescent emission ratio of GO-ATeam1 at 0, 5, 10, and 20 mM ATP. (F) pH-dependent dynamic range of GO-ATeam1 (●) and AT1.03 (○). Dynamic range (%) was defined as follows: dynamic range (%) = ($R_{max}/R_{min} - 1$) × 100. (G) pH-dependent apparent dissociation constant of GO-ATeam1 (●) and AT1.03 (○). All measurements were performed at 37 °C.

firefly luciferase[10] makes it difficult to interpret luminescence data. Because mitochondrial pH changes with mitochondrial activity, we cannot exclude the possibility that such changes, occurring in response to hormonal stimulation, affected luminescence of mitochondrially targeted firefly luciferase. Therefore, a novel pH-resistant system that can monitor ATP together with Ca^{2+} inside single living cells should be necessary for precisely understanding the role of Ca^{2+} in regulating energy metabolism.

Recently, we have developed a series of genetically encoded ATP probes based on the principle of a Förster resonance energy transfer (FRET), called ATeam,[11,12] in which the ε subunit of F_oF_1-ATP synthase is sandwiched between cyan fluorescent protein (CFP) and yellow fluorescent protein (YFP). Specific binding of ATP to the ε subunit[13] in ATeam induces the conformational change of the ε subunit from extended to retracted form,[14] and thereby FRET efficiency in ATeam goes up, allowing researchers, for the first time, to monitor ATP concentrations in living cells at a subcellular spatial resolution. Like most other genetically encoded FRET probes, the ATeam probe uses CFP and YFP as the FRET donor and acceptor, respectively, because the large spectral overlap of CFP emission and YFP absorption is ideal for FRET. The signal of the ATeam probe is almost insensitive to physiological pH in the cytoplasm and mitochondria. CFP/YFP-based FRET probes are rarely used in combination with either inorganic or genetically encoded Ca^{2+} probes. This is because a single CFP/YFP-based FRET probe uses a wide wavelength range that overlaps excitation and/or emission wavelengths of most fluorescent Ca^{2+} probes. Some researchers have reported co-imaging of CFP/YFP-based FRET probes and the

dx.doi.org/10.1021/cb100313n |*ACS Chem. Biol.* 2011, 6, 709–715

most widely used ultraviolet (UV)-excitable inorganic Ca^{2+} probe, fura-2, by narrowing the bandwidth of filters for fluorescence emission to reduce cross-talk between the two fluorescent probes.[15] As a consequence, however, fluorescence intensity from either or both probes is reduced, leading to a significant decrease in the signal-to-noise ratio of the obtained parameters. Monitoring of ATP and Ca^{2+} in a signle cell also has not been achieved with recently developed fluorescent probes for ATP that are based on DNA aptamer[16] or zinc complex.[17] Recently, red-shifted genetically encoded FRET probes, such as those used for studying membrane voltage[18] and Annexin A4,[19] have been developed. The excitation wavelengths of these indicators are far from the UV region. We expected that red-shifted ATP indicators could be used together with UV-excitable fluorescent Ca^{2+} probes with minimal spectral cross-talk between the probes.

RESULTS AND DISCUSSION

Development of the Red-Shifted ATP Probe. To construct an ATeam-type probe with longer excitation and emission wavelengths, we first replaced CFP and YFP with an orange fluorescent protein (OFP), mKOκ,[16] and a variant of *Aequoria* green fluorescent protein (GFP), mEGFP,[20] respectively. Among the orange fluorescent proteins, we chose mKOκ because of its fast maturation, strong photostability, and pH insensitivity. The construct, however, showed an insufficient dynamic range upon ATP binding (data not shown). Optimizing fluorophore orientation by introducing a circular permutation into the fluorescent protein is known to be effective in increasing the dynamic signal range in CFP/YFP-based FRET systems.[21] To expand the dynamic range of the GFP/OFP-based ATP probe, several circularly permuted mEGFPs were examined as FRET donors. Among the constructs, GO-ATeam from the circularly permuted cp173-mEGFP showed the largest dynamic range (emission ratio of GFP and OFP) upon ATP binding. We termed this GFP/OFP-paired ATP probe GO-ATeam1 (Figure 1A,B).

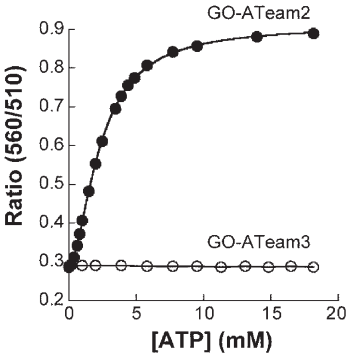

Figure 2. Two GO-ATeam affinity mutants. ATP titration curve of GO-ATeam2 (●) and GO-ATeam3 (○). The fluorescent emission ratios (560 nm/510 nm) at 37 °C in pH 7.3 buffer were plotted against [ATP]. Excitation wavelength was 470 ± 10 nm.

***In Vitro* Characterization of GO-ATeam.** We examined the properties of purified GO-ATeam1. The dissociation constant (K_d) for MgATP was determined to be 7.1 mM at 37 °C and pH 7.3 (Figure 1C). This value is 2-fold higher than the K_d of AT1.03 (3.3 mM), which is based on CFP and YFP. This result suggests that not only the ε subunit but also the interaction between fluorescent proteins could affect the K_d of the ATeam probe. Interaction between GO-ATeam1 and MgATP was completely reversible (Supplementary Figure 1). From kinetic analyses, k_{on} and k_{off} of GO-ATeam1 for MgATP were estimated to be 4.6×10^{-3} M^{-1} s^{-1} and 1.3×10^{-1} s^{-1}, respectively (Figure 1D). We also examined pH-dependency of GO-ATeam1 (Figure 1E−G). The dynamic range of the OFP/GFP ratio change in GO-ATeam was almost insensitive to pH in the range surveyed (6.3−8.3; Figure 1F). This characteristic is in contrast to the original CFP/YFP-based ATeam (AT1.03). The dynamic range of the YFP/CFP ratio change in AT1.03 decreases below pH 7,[11] probably because the CFP quantum yield and YFP absorption, both of which are involved in FRET efficiency, are sensitive to acidic pH.[22] K_d value for ATP of GO-ATeam1 increases from pH 6 to pH 7, and is almost constant above pH 7 (Figure 1G). This means that small pH changes do not affect the fluorescent signal in the cytoplasm (pH ~7.4) and mitochondria (pH ~8.0) under physiological conditions. The reason why acidic pH affects the K_d of GO-ATeam1 is not clear. For comparison purposes, we constructed two GO-ATeam variants with different affinities to MgATP, as in previous studies;[11] GO-ATeam2 constructed from a mutant ε (M60Y/G131E/K132M/133K) showed higher affinity, with K_d of 2.3 mM at 37 °C and pH 7.3 (Figure 2). GO-ATeam3 from ε(R122K/R126K), the binding ability of which is disrupted, did not respond to MgATP (Figure 2).

Monitoring ATP Depletion with GO-ATeam in Living Cells. GO-ATeam1 was successfully expressed in cultured mammalian cells and was localized to the cytoplasm when no targeting sequence was added. To confirm that the GO-ATeam probe

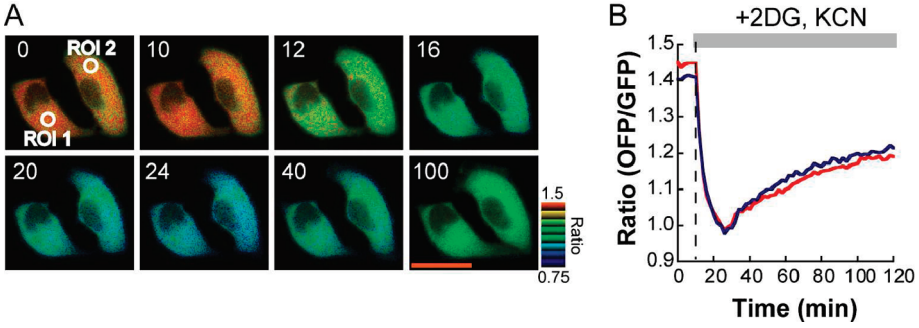

Figure 3. Using GO-ATeam to monitor ATP levels in HeLa cells. GO-ATeam1 was expressed in the cytoplasm of HeLa cell. (A) Sequential images of OFP/GFP emission ratio (pseudocolored) in HeLa cells expressing GO-ATeam1. At time = 10 min, 10 mM 2-deoxyglucose (2DG) and 1 mM KCN were added. The number in the top left corner in each image represents elapsed time (in min). Scale bar = 20 μm. (B) Time course of OFP/GFP emission ratio inside ROI-1 (red line) and ROI-2 (blue line).

dx.doi.org/10.1021/cb100313n |*ACS Chem. Biol.* 2011, 6, 709–715

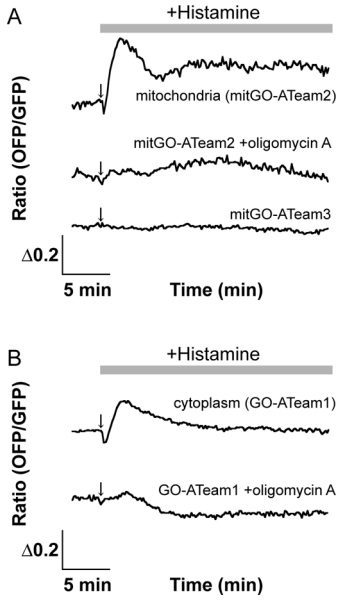

Figure 4. Using GO-ATeam to monitor ATP dynamics in histamine-stimulated single HeLa cells. (A) Dynamics of mitochondrial ATP level. Typical time courses from single cells of the emission ratios of (from top) mitGO-ATeam2, mitGO-ATeam2 in the presence of oligomycin A (1 μg/mL, added before imaging), and mitGO-ATeam3. Histamine was added to a final concentration of 100 μM (indicated by arrow). (B) Dynamics of cytoplasmic ATP level. Typical time courses from single cells of the emission ratio of GO-ATeam1 (top) and GO-ATeam1 in the presence of oligomycin A (1 μg/mL, added before imaging) (bottom).

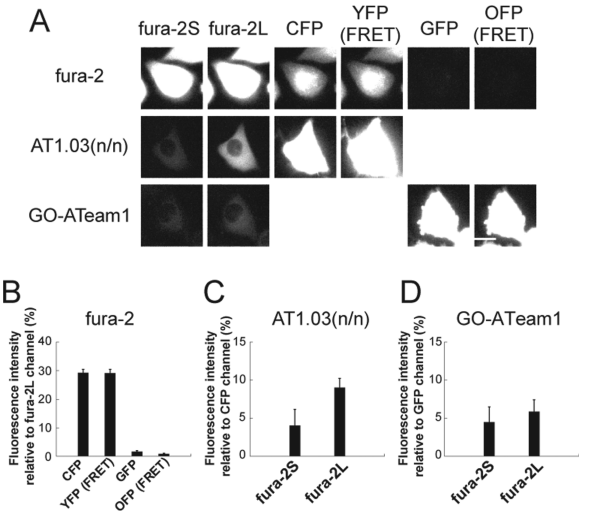

Figure 5. Bleed-through of fura-2, ATeam, and GO-ATeam fluorescence emission into other fluorescence channels. (A) Fluorescence images in fura-2S, fura-2L, CFP, YFP (FRET), GFP, and OFP (FRET) channels of HeLa cells that were loaded with fura-2 (top row), expressed AT1.03(n/n)[12] (middle row), or expressed GO-ATeam1 (bottom row). Scale bar = 20 μm. (B) Bleed-through of fura-2 emission. Fluorescence intensities of fura-2-loaded HeLa cells in the CFP, YFP (FRET), GFP, and OFP (FRET) channels relative to that in the fura-2L channel (N = 8). (C) Bleed-through of ATeam emission. Fluorescence intensities of AT1.03(n/n)-expressing HeLa cells in the fura-2S and fura-2L channels relative to that in the CFP channel (N = 13). (D) Bleed-through of GO-ATeam emission. Fluorescence intensities of GO-ATeam1-expressing HeLa cells in the fura-2S and fura-2L channels relative to that in the GFP channel (N = 8).

can sense intracellular ATP levels like AT1.03 does, we conducted a time course measuring the OFP/GFP emission ratio in HeLa cells expressing GO-ATeam1 while inhibiting cellular ATP synthesis with 2-deoxyglucose (2DG) and KCN, which inhibit glycolysis and oxidative phosphorylation, respectively. Figure 3A shows sequential wide-field images of the pseudocolored OFP/GFP emission ratio. After addition of the inhibitors, the OFP/GFP emission ratio rapidly decreased and, then, gradually recovered (Figure 3B), as previously observed in CFP/YFP-based ATeam measurements.[11] The recuperation of cytoplasmic [ATP] ($[ATP]_c$) would be the result of a cellular response to a large decrease of $[ATP]_c$.

Elevation of Cytoplasmic and Mitochondrial ATP Levels by Histamine. Next, we attempted to visualize the elevation in $[ATP]_m$ induced by phermaceutical stimulation using GO-ATeam. Considering that $[ATP]_m$ of HeLa cell is lower than $[ATP]_c$ in a normal culture condition,[11] GO-ATeam2 was targeted to mitochondrial matrix (mitGO-ATeam2). The OFP/GFP ratio increased immediately after histamine addition (final concentration 100 μM). In a control experiment, GO-ATeam3 was also targeted to the mitochondria, and the OFP/GFP ratio was measured. As expected, it did not significantly respond to the histamine stimulus (Figure 4A). Thus, the elevation in the emission ratio of mitGO-ATeam2 is not due to artifacts, such as pH changes or other microscopic environmental changes. When cells were pretreated with oligomycin A, a specific inhibitor of mitochondrial F_oF_1-ATP synthase, the OFP/GFP ratio of mitGO-ATeam2 did not change upon histamine stimulation (Figure 4A), suggesting that the F_oF_1-ATP synthase is directly responsible for the elevation in $[ATP]_m$. $[ATP]_c$ also increased upon histamine stimulation, which was observed as an increase in the OFP/GFP emission ratio of GO-ATeam1 (Figure 4B). In contrast to $[ATP]_m$, $[ATP]_c$ returns to near basal levels within 10 min after the initial increase. In the presence of oligomycin A, histamine-induced increase in $[ATP]_c$ was almost suppressed and declination of $[ATP]_c$ was observed (Figure 4B). These results clearly confirm that histamine stimulation activates mitochondrial ATP synthesis, leading to the increase in both $[ATP]_m$ and $[ATP]_c$ and suggest that the increased ATP consumption in cytoplasm is compensated by the increased supply of ATP from mitochondria.

Co-imaging ATP and Ca^{2+} in a Single Cell. $[ATP]_m$ and $[Ca^{2+}]$ were imaged together in single cells in order to investigate the time correlation of the histamine-induced dynamics of these factors. For intracellular Ca^{2+} imaging, fura-2, the most widely used Ca^{2+} indicator, was employed. The excitation peak of fura-2 shifts from 380 to 340 nm with Ca^{2+} binding. Therefore, $[Ca^{2+}]$ can be imaged as the fluorescence ratio of the two excitations. Bleed-through of fura-2 fluorescence into CFP, YFP (FRET), GFP, and OFP (FRET) channels and those of the original ATeam and GO-ATeam fluorescence into the fura-2 channels were examined to evaluate the effectiveness of the red-shifted property of GO-ATeam. The fluorescence of fura-2 significantly bled through into the CFP and YFP (FRET) channels (Figure 5). On the other hand, the bleed-through into GFP and OFP (FRET) channels were negligible (Figure 5). The bleed-through of GO-ATeam fluorescence into the fura-2 channel was about 5% of the fluorescence in the GFP channel, although that of ATeam fluorescence into the fura-2 channel was close to 10%. Therefore, fluorescence cross-talk between GO-ATeam and fura-2 is negligible, unlike between ATeam and fura-2.

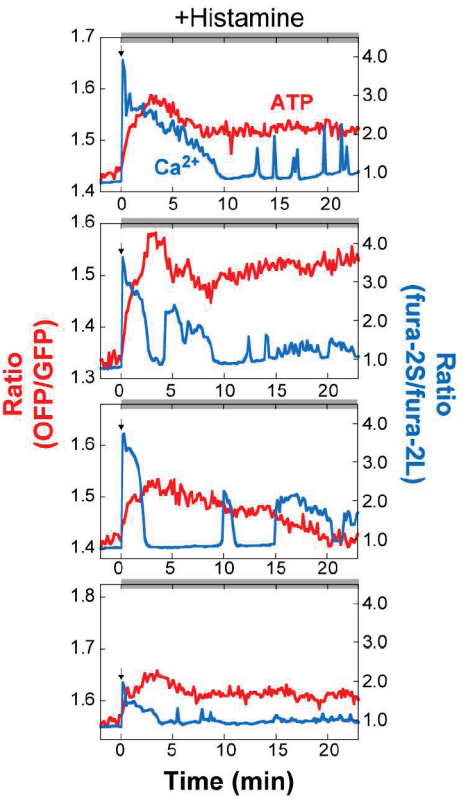

Figure 6. Monitoring of mitochondrial ATP together with cytoplasmic Ca^{2+} in histamine-stimulated single HeLa cells. Fura-2 was loaded into HeLa cells expressing mitGO-ATeam2. Time courses of mitGO-ATeam2 (red line) and fura-2 (blue line) emission ratios from different single cells are shown. Histamine was added at the final concentration of 100 μM at time = 0 min.

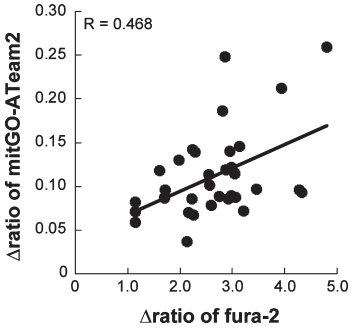

Figure 7. Correlation between $[Ca^{2+}]$ and $[ATP]_m$ increments. Maximum $[Ca^{2+}]$ (excitation ratio of fura-2) and $[ATP]_m$ (emission ratio of mitGO-ATeam2) peaks of individual cells after histamine stimulation were plotted (N = 34). The line represents a linear fitting of the data.

We loaded fura-2 into HeLa cells expressing mitGO-ATeam2 to monitor both $[Ca^{2+}]$ and $[ATP]_m$ dynamics in single cells. In the preliminary imaging, we could obtain a trace of fura-2 signal similar to those reported previously.[23] However, we found that orange emission of mKOκ was converted to green by the UV illumination for fura-2 excitation and that the emerged green fluorescence was photobleached by illumination with blue light for mitGO-ATeam2 excitation (see Supporting Information and Supplementary Figure 2). As a result, the OFP/GFP ratio of mitGO-ATeam2 significantly dropped down without any stimulation when a strong UV

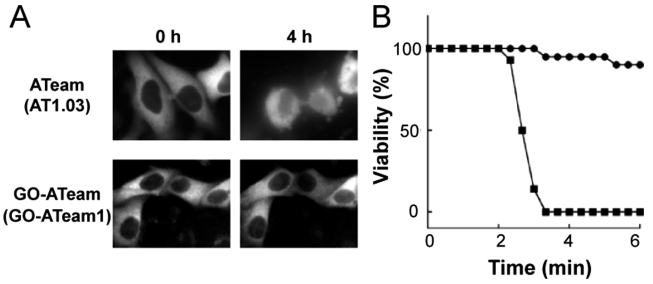

Figure 8. Phototoxicity of GO-ATeam excitation. (A) Fluorescence images of HeLa cells that expressed either AT1.03 (top) or GO-ATeam1 (bottom) exposed to strong excitation light under the microscope. Wavelength used are 427 nm for AT1.03 and 483 nm for GO-ATeam1. Exposure time was 1 s per minute. See Methods for details. (B) Phototoxicity of strong excitation light. Cells were exposed to strong excitation light as in panel A. Viability of cells (N = 14 for AT1.03, 21 for GO-ATeam1) was examined from fluorescence images, where cells with shrunken morphology were regarded as dead. (■) CFP excitation; (●) GFP excitation.

light was used for fura-2 excitation (Supplementary Figure 3). To prevent this artifct, we minimized the power of UV light such that we can obtain sufficient fura-2 signal while photoconversion of mKOκ is negligible. (see Methods and Supporting Information for details). For all cells examined (N = 34), both $[ATP]_m$ and $[Ca^{2+}]$ increased upon histamine stimulation. However, the dynamics of these factors are quite different (Figure 6). Histamine induced acute $[Ca^{2+}]$ elevation inside the cells, which peaked within 1 min after histamine stimulation. Then, intracellular $[Ca^{2+}]$ gradually decreased within 10 min and, in most of cells, started to oscillate (Figure 6, blue lines). In contrast, the increase in $[ATP]_m$ was much slower than the rise in $[Ca^{2+}]$, reaching maximum levels later than 2 min after addition of histamine. The $[ATP]_m$ increase was maintained for more than 20 min (Figure 6, red line). This slower response of $[ATP]_m$ than $[Ca^{2+}]$ cannot be attributed to the inherent response of GO-ATeam and fura-2, beacause the time required for FRET change (inverse of k_{obs}, Figure 1D) of GO-ATeam is shorter than 10 s, even though fura-2 can respond to Ca^{2+} much more quickly ($k_{on} \approx 5 \times 10^8$ M^{-1} s^{-1}, $k_{off} \approx 84$ s^{-1}).[24] Indirect activation of PDH by Ca^{2+}, as Ca^{2+} activates PDH phosphatase that converts the inactive phosphorylated PDH to the active dephosphorylated PDH [3] might account for the slow response of $[ATP]_m$. If PDH phosphorylation occurs slowly, PDH would retain high activity even after $[Ca^{2+}]$ returned to basal levels. To determine the effects of Ca^{2+} on mitochondrial ATP synthesis in each cell, maximum $[ATP]_m$ and $[Ca^{2+}]$ increases above basal levels (prior to histamine addition) were compared. Although the increments by which both $[ATP]_m$ and $[Ca^{2+}]$ increased varied among cells, the increment of $[ATP]_m$ was apparently correlated with that of $[Ca^{2+}]$ (Figure 7). These results indicate that individual cells have a system to control mitochondrial ATP synthesis in accordance with elevated Ca^{2+} levels in order to maintain ATP concentrations inside the cells.

Reduced Phototoxicity of GO-ATeam Excitation Light. In fluorescent live cell imaging, phototoxicity of the excitation light is a frequent problem. Phototoxicity of blue light, which is used for exciting GO-ATeam, was compared to that of violet light, used with the original CFP/YFP-based ATeam. When HeLa cells were irradiated every 1 min for 1 s by violet light (from a 75 W xenon lamp through a 427/10 nm filter, attenuated to 25% with ND filter), all cells died within 3 h as assessed by nuclear

dx.doi.org/10.1021/cb100313n |ACS Chem. Biol. 2011, 6, 709–715

condensation. On the other hand, we did not observe any dead cell after the 3-h observation when blue light (from a 75 W xenon lamp through a 482/18 nm filter, attenuated to 25% with ND filter) was used instead of violet light (Figure 8). This result indicates that the use of GO-ATeam can greatly reduce the phototoxicity of the excitation light, making GO-ATeam more suitable for long-term observation of intracellular ATP level than the original ATeam probe.

Conclusions and Outlook. CFP and YFP are the most widely used fluorescent protein combination for genetically encoded FRET probes.[25] However, this combination limits the co-imaging with UV-excitable fluorescent indicators such as fura-2, and the violet light used for excitation potentially damages cells. In this paper, we replaced CFP and YFP in the previously reported genetically encoded ATP indicators (ATeams) with OFP (mKOκ) and GFP (cp173-mEGFP). Because GFP is much less excitable by UV light than CFP, this novel GFP/OFP-based genetically encoded ATP probe, GO-ATeam, is fully compatible with fura-2. This probe allowed us to confirm that Ca^{2+} signaling enhances mitochondrial ATP synthesis. Because Ca^{2+} is involved in many other cellular processes, fura-2 must be used together with genetically encoded fluorescent indicators to monitor cellular events together with the changes in intracellular $[Ca^{2+}]$. CFP and YFP used in other CFP/YFP-based FRET probes might be replaced by the two fluorescent proteins used in this study in order to use them with fura-2 or other UV-excitable fluorescent indicators.

The use of fluorescent proteins with longer excitation and emission wavelengths has other advantages. First, longer-wavelength excitation is significantly less phototoxic to cells. Therefore, this probe will allow long-term imaging of live cells and can reduce artifacts due to phototoxicity. Second, the longer wavelength emission is more appropriate for imaging thick biological samples, such as tissues, because transmission of longer wavelengths light is less perturbed.

In conclusion, the red-shifted genetically encoded ATP probes developed in this study will be suitable not only for imaging of ATP with Ca^{2+} in single cells but also for long-term ATP imaging in thick samples, such as tissues and small organisms.

METHODS

Chemicals. DNA polymerase and DNA ligation kit were purchased from TaKaRa Bio. Oligonucleotides were from Hokkaido System Science. Restriction endonucleases were obtained from Roche Diagnostics. ATP and histamine were from Sigma-Aldrich. Fura-2-AM was purchased from Dojindo Laboratories. Other chemical reagents were from Wako Pure Chemicals unless otherwise noted.

Plasmid Construction. The plasmid encoding mKO2 (pmKO2-S1) cDNA was purchased from Molecular Biology Laboratory. The cDNA for cp173-mEGFP was constructed from the mEGFP plasmid (a kind gift from Dr. Akira Kitamura) using polymerase chain reaction (PCR). The cDNAs encoding mKOκ, *Bacillus subtilis* ε subunit, and cp173-mEGFP were amplified by PCR and then ligated into a single construct. Ligated DNA was then ligated into the *Xho*I and *Hin*dIII sites of pRSET-B vector to obtain pRSET-GO-ATeam for expressing GO-ATeam in *Escherichia coli* and into *Xho*I-*Hin*dIII sites of pcDNA3.1(−) (Invitrogen) to obtain pcDNA-GO-ATeam for mammalian expression.

Purification of GO-ATeam from *E. coli*. *E. coli* strain JM109 (DE3) carrying the GO-ATeam plasmid was cultured in LB medium at 28 °C for 12 h. Protein expression was induced by adding 10 μM isopropyl-β-thiogalactopyranoside and culturing at 23 °C for 36 h. Cells were collected by centrifugation, suspended in buffer A (100 mM sodium phosphate, pH 8.0; 200 mM sodium chloride; 10 mM imidazole-HCl), and then disrupted by sonication. After centrifugation, the supernatant was applied to a Ni-NTA column (QIAGEN) equilibrated with buffer A. After washing the column with buffer A, the protein was eluted by increasing the imidazole concentration to 200 mM. Fractions containing GO-ATeam were concentrated and then applied to Superdex 200 gel-filtration columns (GE Healthcare) equilibrated with 20 mM Tris-HCl (pH 8.0), 150 mM NaCl, and 1 mM EDTA-Na. After adding glycerol to a final concentration of 20%(w/v), the purified GO-ATeam protein was stored at −80 °C until use.

Measurement of Fluorescence *in Vitro*. The fluorescence of purified GO-ATeam proteins was investigated using buffer B (50 mM MOPS-KOH, pH 6.3−7.5, or HEPES-KOH, pH 7.7−8.3; 50 mM KCl; 0.5 mM $MgCl_2$; and 0.05%(w/v) Triton X-100) using an FP-6500 spectrofluorometer (Jasco) at 37 °C. To obtain the fluorescence spectra, cp173-mEGFP was excited with 470 ± 10 nm light, and emission from 490 to 600 nm was scanned. For kinetic measurements, cp173-mEGFP was excited with 470 ± 2.5 nm light, and emission at 510 ± 10 nm was monitored every 0.5 s by adding MgATP at a specific time point. Rates of fluorescence change (k_{obs}) were estimated by fitting fluorescence traces with single exponential equations. ATP was mixed with equimolar $MgCl_2$ to obtain MgATP complex.

Cell Culture, Transfection, and Fura-2 Loading. HeLa cells were obtained from the Japanese Collection of Research Bioresources and maintained in Dulbecco's modified Eagle's medium (DMEM, Sigma) supplemented with 10% fetal bovine serum (FBS; Invitrogen). Cells were plated on a collagen-coated glass-bottom dish (0.17 mm thickness, Fine Plus International Ltd., Kyoto, Japan) and transfected with the plasmid encoding GO-ATeam cDNA by using FuGENE6 transfection reagent (Roche Diagnostics). Between 1 and 2 days after transfection, cell cultured in phenol red-free DMEM were subjected to imaging. For Ca^{2+} imaging, 0.5−1.0 μM fura-2-AM was loaded onto HeLa cells in modified Krebs-Ringer buffer (20 mM HEPES, 125 mM NaCl, 5 mM KCl, 1 mM Na_3PO_4, 1 mM $MgSO_4$, 1 mM $CaCl_2$, 5.5 mM glucose, and 1 mM pyruvate, adjusted to pH 7.3) supplemental with 0.5× concentration of PowerLoad (Invitrogen) for 10 min at RT, and then 10% FBS was added to the medium. After incubation for 3 min at RT, the medium was changed to modified Krebs-Ringer buffer.

Microscopy. Cells were visualized with a Nikon TE2000-E inverted microscope (Nikon Corp., Tokyo, Japan) using the Plan Fluor 40×, 1.30 numerical aperture, oil-immersion objective lens (Nikon). The filters used for dual-emission ratio imaging of GO-ATeam were purchased from Semrock (Rochester, NY) and included an FF01-482/18 excitation filter, an FF495-DiO2 dichroic mirror, and 2 emission filters (FF01-520/35 for GFP and FF01-562/40 for OFP).

For co-imaging of mitGO-ATeam2 and fura-2, cells were visualized with a Nikon Ti-E inverted microscope (Nikon) using UApo/340 40×, 1.35 numerical aperture, oil-immersion objective lens (Olympus). The filters used for dual emission ratio of mitGO-ATeam2 were purchased from Nikon and Semrock. These included a 472/30 nm excitation filter, a 495 nm dichroic mirror (GFP-HQ, Nikon), and 2 emission filters (FF01-520/35 for GFP and FF01-580/23 for OFP, Semrock). The filters used for dual-excitation ratio imaging of fura-2 were purchased from Semrock. These included FF01-340/26 for shorter excitation wavelengths of fura-2 (fura-2S), FF01-387/11 for longer excitation wavelengths of fura-2 (fura-2L), an FF409-DiO2 dichroic mirror, and an FF01-510/84 emission filter. The emission and excitation filters were alternated by using a filter exchanger. Cells were illuminated using a mercury lamp thorough 1% and 12.5% neutral density (ND) filters. Fluorescence emissions from mitGO-ATeam2 and fura-2 were imaged by using a cooled charge-coupled device (CCD) camera (ORCA-R2; Hamamatsu Photonics, Hamamatsu, Japan); the exposure times were 500 ms for GFP and OFP images, and 100 ms for fura-2S and fura-2L images. The cells were maintained on the microscope at 37 °C by using a

stage-top incubator (Tokai Hit, Fujinomiya, Japan). Image analysis was performed using MetaMorph (Molecular Devices, Sunnyvale, CA). The OFP/GFP and fura-2S/fura-2L emission ratios were calculated by dividing an OFP intensity with a GFP intensity, and a fura-2S intensity with a fura-2L intensity within a region of interest (ROI).

■ ASSOCIATED CONTENT

Supporting Information. This material is available free of charge *via* the Internet at http://pubs.acs.org.

■ AUTHOR INFORMATION

Corresponding Author

*E-mail: imamura@lif.kyoto-u.ac.jp, hnoji@appchem.t.u-tokyo.ac.jp.

■ ACKNOWLEDGMENT

We are indebted to all of the members of the Noji and Nagai Laboratory for valuable discussions and advice. We would like to thank the Nikon imaging Center at Hokkaido University for imaging equipments and software. This work was supported by Grants-in-Aid for Scientific Research 18074005, and 18201025 (to H.N.), by Grant-in-Aid for Young Scientists 22687011 (to H. I.), and The Cooperative Research Program of "Network Joint Research Center for Materials and Devices" (to H.N. and T.N.) from the Ministry of Education, Culture, Sports, Science, and Technology of Japan, and Precursory Research for Embryonic Science (to H.I.) from Japan Science and Technology Agency.

■ REFERENCES

(1) Balaban, R. S. (2009) The role of Ca^{2+} signaling in the coordination of mitochondrial ATP production with cardiac work. *Biochim. Biophys. Acta 1787*, 1334–1341.

(2) Hansford, R. G., and Chappell, J. B. (1967) The effect of Ca^{2+} on the oxidation of glycerol phosphate by blowfly flight-muscle mitochondria. *Biochem. Biophys. Res. Commun. 27*, 686–692.

(3) Denton, R. M., Randle, P. J., and Martin, B. R. (1972) Stimulation by calcium ions of pyruvate dehydrogenase phosphate phosphatase. *Biochem. J. 128*, 161–163.

(4) Denton, R. M., Richards, D. A., and Chin, J. G. (1978) Calcium ions and the regulation of NAD^+-linked isocitrate dehydrogenase from the mitochondria of rat heart and other tissues. *Biochem. J. 176*, 899–906.

(5) McCormack, J. G., and Denton, R. M. (1979) The effects of calcium ions and adenine nucleotides on the activity of pig heart 2-oxoglutarate dehydrogenase complex. *Biochem. J. 180*, 533–544.

(6) McCormack, J. G., Halestrap, A. P., and Denton, R. M. (1990) Role of calcium ions in regulation of mammalian intramitochondrial metabolism. *Physiol. Rev. 70*, 391–425.

(7) Trenker, M., Malli, R., Fertschai, I., Levak-Frank, S., and Graier, W. F. (2007) Uncoupling proteins 2 and 3 are fundamental for mitochondrial Ca^{2+} uniport. *Nat. Cell Biol. 9*, 445–452.

(8) Perocchi, F., Gohil, V. M., Girgis, H. S., Bao, X. R., McCombs, J. E., Palmer, A. E., and Mootha, V. K. (2010) MICU1 encodes a mitochondrial EF hand protein required for Ca^{2+} uptake. *Nature 467*, 291–296.

(9) Jouaville, L. S., Pinton, P., Bastianutto, C., Rutter, G. A., and Rizzuto, R. (1999) Regulation of mitochondrial ATP synthesis by calcium: evidence for a long-term metabolic priming. *Proc. Natl. Acad. Sci. U.S.A. 96*, 13807–13812.

(10) Seliger, H. H., and McElroy, W. D. (1964) The colors of firefly bioluminescence: enzyme configuration and species specificity. *Proc. Natl. Acad. Sci. U.S.A. 52*, 75–81.

(11) Imamura, H., Huynh Nhat, K. P., Togawa, H., Saito, K., Iino, R., Kato-Yamada, Y., Nagai, T., and Noji, H. (2009) Visualization of ATP levels inside single living cells with fluorescence resonance energy transfer-based genetically encoded indicators. *Proc. Natl. Acad. Sci. U. S.A. 106*, 15651–15656.

(12) Kotera, I., Iwasaki, T., Imamura, H., Noji, H., and Nagai, T. (2010) Reversible dimerization of Aequorea victoria fluorescent proteins increases the dynamic range of FRET-based indicators. *ACS Chem. Biol. 5*, 215–222.

(13) Kato-Yamada, Y., and Yoshida, M. (2003) Isolated ε subunit of thermophilic F_1-ATPase binds ATP. *J. Biol. Chem. 278*, 36013–36016.

(14) Yagi, H., Kajiwara, N., Tanaka, H., Tsukihara, T., Kato-Yamada, Y., Yoshida, M., and Akutsu, H. (2007) Structures of the thermophilic F_1-ATPase ε subunit suggesting ATP-regulated arm motion of its C-terminal domain in F_1. *Proc. Natl. Acad. Sci. U.S.A. 104*, 11233–11238.

(15) Carlson, H. J., and Campbell, R. E. (2009) Genetically encoded FRET-based biosensors for multiparameter fluorescence imaging. *Curr. Opin. Biotechnol. 20*, 19–27.

(16) Özalp, V. C., Pedersen, T. R., Nielsen, L. J., and Olsen, L. F. (2010) Time-resolved measurements of intracellular ATP in the yeast *Saccharomyces cerevisiae* using a new type of nanobiosensor. *J. Biol. Chem. 285*, 37579–37588.

(17) Kurishita, Y., Kohira, T., Ojida, A., and Hamachi, I. (2010) Rational design of FRET-based ratiometric chemosensors for in vitro and in cell fluorescence analyses of nucleoside polyphosphates. *J. Am. Chem. Soc. 132*, 13290–13299.

(18) Tsutsui, H., Karasawa, S., Okamura, Y., and Miyawaki, A. (2008) Improving membrane voltage measurements using FRET with new fluorescent proteins. *Nat. Methods 5*, 683–685.

(19) Piljic, A., and Schultz, C. (2008) Simultaneous recording of multiple cellular events by FRET. *ACS Chem. Biol. 3*, 156–160.

(20) Zacharias, D. A., Violin, J. D., Newton, A. C., and Tsien, R. Y. (2002) Partitioning of lipid-modified monomeric GFPs into membrane microdomains of live cells. *Science 296*, 913–916.

(21) Nagai, T., Yamada, S., Tominaga, T., Ichikawa, M., and Miyawaki, A. (2004)Expanded dynamic range of fluorescent indicators for Ca^{2+} by circularly permuted yellow fluorescent proteins. *Proc. Natl. Acad. Sci. U.S.A. 101*, 10554–10559.

(22) Miyawaki, A., and Tsien, R. Y. (2000) Monitoring protein conformations and interactions by fluorescence resonance energy transfer between mutants of green fluorescent protein. *Methods Enzymol. 327*, 472–500.

(23) Sauvé, R., Diarra, A., Chahine, M., Simoneau, C., Morier, N., and Roy, G. (1991) Ca^{2+} oscillations induced by histamine H1 receptor stimulation in HeLa cells: Fura-2 and patch clamp analysis. *Cell Calcium 12*, 165–176.

(24) Jackson, A. P., Timmerman, M. P., Bagshaw, C. R., and Ashley, C. C. (1987) The kinetics of calcium binding to fura-2 and indo-1. *FEBS Lett. 216*, 35–39.

(25) VanEngelenburg, S. B., and Palmer, A. E. (2008) Fluorescent biosensors of protein function. *Curr. Opin. Chem. Biol. 12*, 60–65.